

Universal elastic and plastic effects in the particle caging of polymers and glassforming liquids

F. Puosi

Dipartimento di Fisica “Enrico Fermi”, Università di Pisa, Largo B.Pontecorvo 3, I-56127 Pisa, Italy

D. Leporini*

*Dipartimento di Fisica “Enrico Fermi”, Università di Pisa, Largo B.Pontecorvo 3, I-56127 Pisa, Italy and
IPCF-CNR, UOS Pisa, Italy*

(Dated: August 24, 2011)

The peculiar intermittency of the single-particle motion close to the glass transition follows from the continuous (elastic) trapping into the neighbors cage and the subsequent (plastic) escape. The universal correlation of the residual elasticity and the incipient plasticity on the picosecond time scale with the cage restructuring is revealed by extensive simulations and validated by comparison with experimental data spanning about eighteen decades in relaxation time and a wide range of fragilities. Universality is lost on sub-picosecond time scales where the elastic energy due to non-affine microscopic displacements is still stored.

PACS numbers: 64.70.P-, 62.20.de, 66.20.-d

If liquids avoid crystallization during cooling or compression, their viscosity grows by orders of magnitude and they finally freeze into a microscopically disordered solid-like state, a glass [1]. On approaching the glass transition (GT), particles tend to be trapped in transient cages formed by their nearest neighbours. The particles rattle about in the cage on picosecond time scales and are later released with average escape time, or structural relaxation time τ_α , increasing from a few picoseconds to thousands of seconds through the transition [1, 2]. After the release, particles undergo short periods of larger displacement terminated by a new trapping [3, 4]. Owing to this stop-and-go process, the single-particle dynamics becomes strongly intermittent [5].

The fast rattling motion of particles during the trapping periods has strong analogies with the oscillatory *elastic* behaviour of particles in crystalline and amorphous solids. Several “elastic” models of the structural relaxation and the viscous flow have been developed since long time ago [6] and over the years (for excellent reviews see [7, 8]). See also recent experimental [9, 10], theoretical [11, 12] and computational [10, 13, 14] work in a wide class of materials including colloids, liquids, polymers and metallic alloys. The key prediction of the elastic models is that the viscosity η and the structural relaxation are activated with energy cost, due to the cage breaking, being proportional to the instantaneous, or infinite-frequency, shear modulus G_∞ [7, 8]:

$$\log \eta / \eta_0, \log \tau_\alpha / \tau_0 = \frac{\Delta E}{k_B T}; \quad \Delta E = G_\infty V^* \quad (1)$$

where V^* is an activation volume with negligible temperature dependence. Eq.1 relies on two underlying assumptions: i) only the trapping period, and not the subsequent escape process, is pertinent to relaxation, ii) continuum elasticity theory applies to microscopic length scales as well. Both assumptions are debatable in that: i) departing from GT, trapping is less effective and the role of the escape process increases, ii) after a homogeneous large-scale deformation, the discreteness of the matter leads to inhomogeneous, non-affine fast displacements of the particles within the cage [15, 16] with the

subsequent drop of the modulus from G_∞ to the finite frequency plateau (or “relaxed”) modulus G_r [17]. Virtually, all the experiments validating Eq.1 actually measure G_r since the elastic response is probed at frequencies much lower than the THz range where the crossover from G_r to G_∞ is located [11]. Then, the approximation $G_\infty \simeq G_r$ is usually assumed [7–10, 12]. Surprisingly, in spite of the delicate conjectures underlying the popular elastic models a thorough test of Eq.1 is missing.

The present Letter reports striking evidence by extensive molecular-dynamics (MD) simulations that G_r , but not G_∞ , exhibits strong universal correlations with the short-time (picosecond) mean square displacement (ST-MSD) of the kinetic unit $\langle u^2 \rangle$. The latter quantity, which will be related to specific details of the potential-energy landscape (PEL) [18], reveals a simple picture of the intermittent dynamics expressed by the *quasi-elastic* relation (in reduced MD units):

$$\frac{1}{\langle u^2 \rangle} = \frac{G_r V^*}{k_B T} + \frac{1}{\langle u_\infty^2 \rangle}. \quad (2)$$

It is shown that the first term on the rhs is the inverse ST-MSD during the trapping period, whereas $\langle u_\infty^2 \rangle$ is associated to the incipient escape from the cage. Eq.2 improves the usual *elastic* approximation with $\langle u_\infty^2 \rangle^{-1} = 0$ and $G_r = G_\infty$ [7, 11, 19]. The combination of Eq.2 with previous results [14] predicts the scaling of τ_α , or η , and G_r/T . It is shown that the resulting master curve fits the experimental results over about eighteen decades in relaxation time ($-12 \lesssim \log \tau_\alpha \lesssim 6$) and a wide range of fragilities ($20 \leq m \leq 115$) with *one* adjustable parameter, to be compared with the reported range of validity of Eq. 1 ($-6 \lesssim \log \tau_\alpha \lesssim 2$ [7]) with *two* adjustable parameters (V^* and τ_0 or η_0) and the identification $G_\infty = G_r$.

We performed extensive molecular-dynamics (MD) simulations of a melt of fully-flexible linear chains of M soft spheres (monomers, $N \simeq 2000$ in total) by changing the temperature T , the number density ρ , the chain length and the interacting potential between non-bonded monomers. Details about the model are given elsewhere [14] and summarized in

Supplemental Material (SM) [20] where all the investigated states (~ 100) are also listed. MD results are in reduced units (Boltzmann constant $k_B = 1$).

We start by comparing both the single-particle and the collective dynamics. The former is characterized via the incoherent intermediate scattering function (ISF) $F_s(q, t) = N^{-1} \langle \sum_{j=1}^N \exp\{-i\mathbf{q} \cdot [\mathbf{r}_j(t) - \mathbf{r}_j(0)]\} \rangle$ at q_{max} , the q -vector of the maximum of the static structure factor [2]. The relation $F_s(q_{max}, \tau_\alpha) = 1/e$ defines the structural relaxation time τ_α . The collective dynamics is described by the transient elastic modulus of a volume V , $G(t)$, being expressed by the correlation function:

$$G(t) = \frac{V}{k_B T} \langle \sigma_{xy}(t_0) \sigma_{xy}(t_0 + t) \rangle. \quad (3)$$

σ_{xy} is the off-diagonal component of the stress tensor :

$$\sigma_{xy} = \frac{1}{V} \left(\sum_{i=1}^N \left[m v_{xi} v_{yi} + \frac{1}{2} \sum_{j \neq i} r_{xij} F_{yij} \right] \right) \quad (4)$$

where $v_{\alpha k}$, $F_{\alpha kl}$, $r_{\alpha kl}$ are the α components of the velocity of the k th monomer with mass m , the force between the k th and the l th monomer and their separation, respectively. Note that $G(0) = G_\infty$ [21].

Fig.1 shows the characteristic two-step decay of both $G(t)$ (top) and ISF (bottom). The drop of both $G(t)$ and ISF over times $t \sim 1$, corresponding to few picoseconds in real time [14], follows from the exploration of the cage by the trapped monomer. This results in the fast, large drop of $G(t)$ from G_∞ to G_r , i.e. the plateau height measured by most viscoelastic experiments [11]. It seems proper to deepen the discussion about this point. In crystals with one particle per unit cell under athermal conditions the equality $G_r = G_\infty$ holds [15]. In such a case, the total force acting on each particle, F_{tot} vanishes during the shear strain. Differently, even under athermal conditions, in crystals with multi-atom unit cell [15] and amorphous systems [16] the total force on each particle unbalances ($F_{tot} \neq 0$) after the fast, homogeneous, affine shear strain. At finite temperature the mechanical equilibrium is restored rapidly by the non-affine particle displacements within their cages, leading to considerable loss of elastic energy [16]. Note that the differences between G_r and G_∞ are reduced but not suppressed in the glass for $T < T_g$ since local cage rattling is still present [22].

The fact that $G(t)$ vanishes at $t \sim \tau_\alpha$ (Fig.1 top) shows that the plateau G_r is controlled by the local structure [17]. To provide more insight, the configurations explored by the system via the true dynamics are sampled in time and "quenched" to the so-called inherent structures (IS) by locally minimizing the potential energy in configurational space, i.e. enforcing mechanical equilibrium ($F_{tot} = 0$) [18]. The IS time series defines the "inherent" dynamics of the system. Fig.1 shows that the true and the inherent decay of $G(t)$ differ at very short times but coincide for times longer than $t \sim 1$. This confirms that the initial drop of $G(t)$ follows from mechanical equilibration. The insets of Fig.1(top) provide information

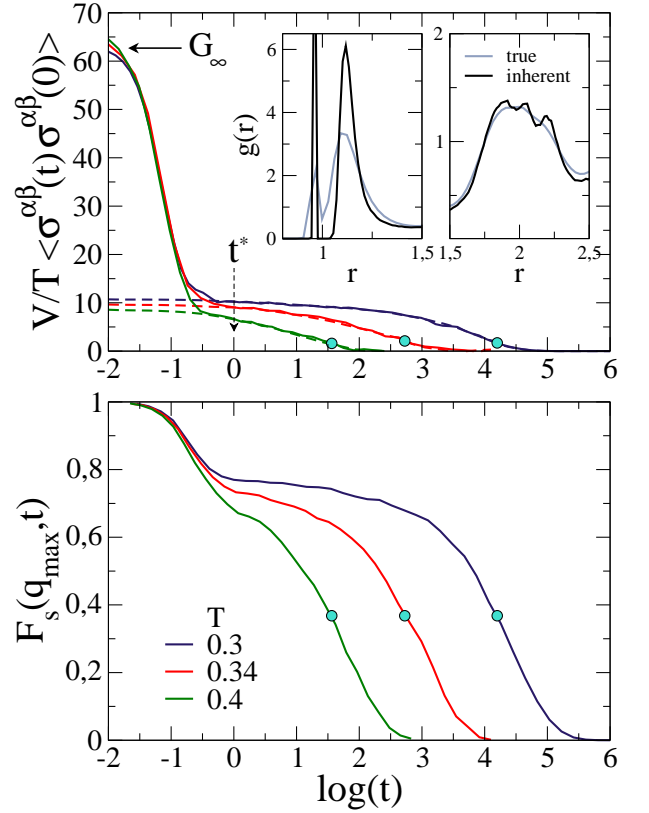


FIG. 1: (Color online) MD results of the relaxation properties of linear chains with $M = 3, \rho = 0.984$ at the indicated temperatures. Non-bonded monomers interact with Lennard-Jones potential [20]. Top Panel: transient elastic modulus $G(t)$. Note that $G(0) = G_\infty$. The relaxed shear modulus is defined by $G_r \equiv G(t^*)$, t^* is defined in the text. Insets show the true and the quenched (inherent) radial pair distribution functions in the regions of the first and the second neighbor shells at $T = 0.3$. The peak at $r \sim 0.97$ corresponds to the adjacent *bonded* monomers. The fine structure of the peak of the second neighbor shell ($1.5 \lesssim r \lesssim 2.5$) is discussed in the text. Bottom Panel: intermediate scattering function $F_s(q_{max}, t)$. Dots mark the structural relaxation time τ_α .

on the IS structures by comparing the actual and the inherent radial distribution functions. The latter, having removed the vibrational cage rattling, is much more detailed. In particular the peak corresponding to the second neighbor shell is split in three sub-peaks at $r \simeq 1.89, 2.05, 2.19$. The side sub-peaks are well-known signatures of local icosahedral order in *atomic* Lennard-Jones liquids at $r \simeq 1.89, 2.15$ [23]. The central sub-peak is characteristic of the present *molecular* system and is assigned to linear trimers of two bonded and one non-bonded monomers (not shown).

The first escapes of the monomer from the cage occur at very short times. By observing the monomer MSD $\langle r^2(t) \rangle$, it was noticed that the quantity $\partial \log \langle r^2(t) \rangle / \partial \log t$ shows a well-defined minimum at $t^* = 1.023$ signaling early detraping (t^* is independent of the physical state in the present model) [14]. We define $\langle u^2 \rangle \equiv \langle r^2(t^*) \rangle$ and $G_r \equiv G(t^*)$

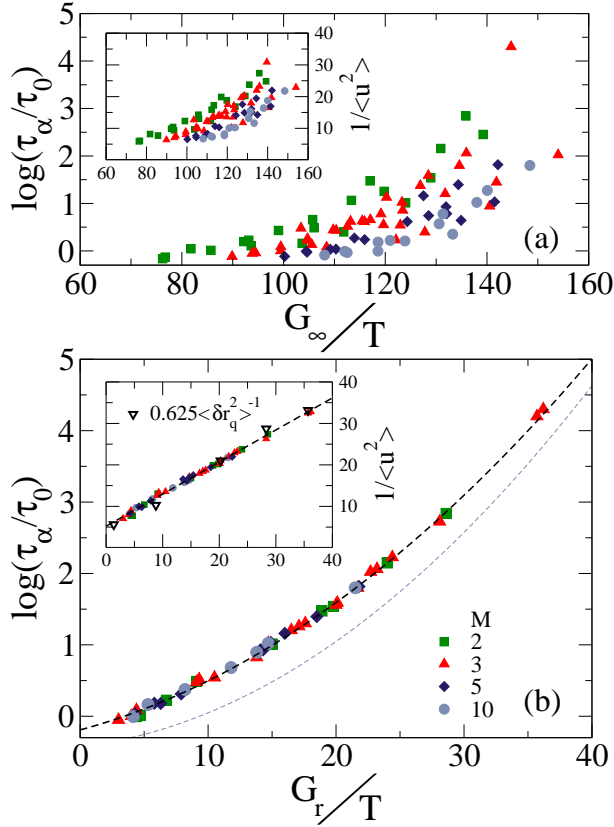


FIG. 2: (Color online) Panel (a): The structural relaxation time τ_α and the ST-MSD $\langle u^2 \rangle$ (inset) versus the ratio G_∞/T from MD simulations. Panel (b): Same as in panel (a) with the reduced elastic modulus G_r . The open triangles and the dashed heavy line in the inset are the inverse return distance $\langle \delta r_q^2 \rangle^{-1}$ of the states in Fig.1 (plus $T = 0.6, 1$) [18] and Eq.2 with $V^* = 0.77(2)$ and $\langle u^2 \rangle_\infty = 0.192(4)$, respectively. The dashed heavy and thin lines in the main panel are the combination of Eq. 5 with Eq.2 by either including or not the term $\langle u^2 \rangle_\infty^{-1}$ of Eq.2, respectively. Note that replacing G_∞ by G_r in Eq.1 leads to a linear master curve differing from the MD results. The investigated states, obtained by changing T, ρ, M and the interacting potential between non-bonded monomers, are listed in SM [20].

as the ST-MSD [14] and the residual elastic modulus (see Fig.1(top)), respectively. It is known that strong correlation exists between the structural relaxation and $\langle u^2 \rangle$ [24], resulting in the universal master curve [14]:

$$\log \tau_\alpha = \alpha + \beta \langle u^2 \rangle^{-1} + \gamma \langle u^2 \rangle^{-2} \quad (5)$$

with $\alpha = -0.424(1)$, $\beta = 2.7(1) \cdot 10^{-2}$, $\gamma = 3.41(3) \cdot 10^{-3}$ in MD units.

We are now in a position to investigate the correlation of the elastic properties with $\langle u^2 \rangle$ and then τ_α . Fig.2 compares the latter quantities with both G_∞ (top) and G_r (bottom). It is quite apparent that G_∞ , the central quantity of the standard elastic models [7, 8], poorly correlates with both the structural relaxation and even $\langle u^2 \rangle$ despite the latter is evaluated at very short times, few picoseconds in real time. Differently, very

high correlations of G_r with both $\langle u^2 \rangle$ and τ_α are observed (Fig.2b). In particular, the inset shows the remarkable linear scaling law, Eq.2 [25]. The constancy of the parameters of Eq. 2, V^* and $\langle u_\infty^2 \rangle$, is ascribed to the limited changes of the local structure due to the high packing of the investigated states [24, 26]. The combination of Eq.2 and Eq.5 yields a quadratic master curve between $\log \tau_\alpha$ and G_r/T which well agrees with the MD results (Fig.2b) and is not recovered by replacing G_∞ with G_r in Eq.1. Fig.2b also shows that $\langle u_\infty^2 \rangle^{-1}$ cannot be neglected in Eq.2, i.e. far from GT the elastic response competes with, i.e. is often interrupted by, the escape process. However, the elastic term dominates close to GT, thus recovering the usual elastic approximation [7, 11, 19].

To provide insight into Eq. 2 we resort to the PEL viewpoint, where IS are grouped to form distinct metabasins (MB) separated by high energy barriers [18]. In this context one sees that the elasticity due to trapping is set by intra-MB dynamics, whereas the trapping release is accounted for by the inter-MB dynamics. More quantitatively, we consider the return distance (squared) $\langle \delta r_q^2 \rangle = N^{-1} \sum_{i=1}^N \langle |\mathbf{r}_i(t) - \mathbf{r}_i^q|^2 \rangle$, involving the separation between the instantaneous and the quenched IS positions, thus providing an estimate of the aperture of that portion of the basin encountered by the trajectories [18]. Remarkably, δr_q^2 , differently from the instantaneous displacement involved in the definition of $\langle u^2 \rangle$, is a *stationary* random variable and then $\langle \delta r_q^2 \rangle$ is a characteristic constant quantity of each physical state. It is found that $\langle \delta r_q^2 \rangle = 0.625 \langle u^2 \rangle$ (Fig.2b, inset), i.e. $\langle u^2 \rangle$ is an excellent surrogate of the return distance (the proportionality constant is close to 0.5, expected for uncorrelated deviations of the instantaneous positions from the IS). This identification allows us to interpret the two terms of Eq. 2, $\langle u_\infty^2 \rangle$ and the "elastic" ST-MSD $k_B T / G_r V^*$ dominating close to GT, as the average MB full width (or approximately the MSD to reach a different MB), and the typical MSD *within* a MB, respectively. As an example, for a binary mixture the typical MSD *within* a MB ($\simeq 6 \cdot 10^{-2}$) and *to reach* a different MB ($\simeq 0.2$) [4] are rather comparable, at the same $\tau_\alpha (\simeq 4 \cdot 10^3)$, to the "elastic" ST-MSD ($\simeq 4.5 \cdot 10^{-2}$), and $\langle u^2 \rangle_\infty \simeq 0.192$ of the monomers, respectively.

Are the MD results robust enough to be compared with the experiments? The fact that Eq.5, assessed in the weakly supercooled regime attainable by MD simulations, holds true down to GT ($\log \tau_{\alpha g} = 13.5 \pm 0.5$, $\langle u_g^2 \rangle = 0.0166$) evidences that the relevant information on the coupling between the intermittent motion and the long-time relaxation is present at high temperatures [14]. This motivates us to extend the validity of Eq.2 down to GT and get the ratio G_{rg}/T_g since $\langle u_g^2 \rangle = 0.0166$ [14]. By plugging Eq. 2 into Eq. 5 and defining the reduced variable $X = G_r T_g / (G_{rg} T)$, one obtains a quadratic form as candidate for the universal master curve:

$$\log \tau_\alpha = \delta + \epsilon X + \phi X^2 \quad (6)$$

with $\delta = -11.70(1)$, $\epsilon = 3.4(2)$, $\phi = 10.3(8)$ (δ is set so as to get the familiar $\log \tau_\alpha = 2$ at GT).

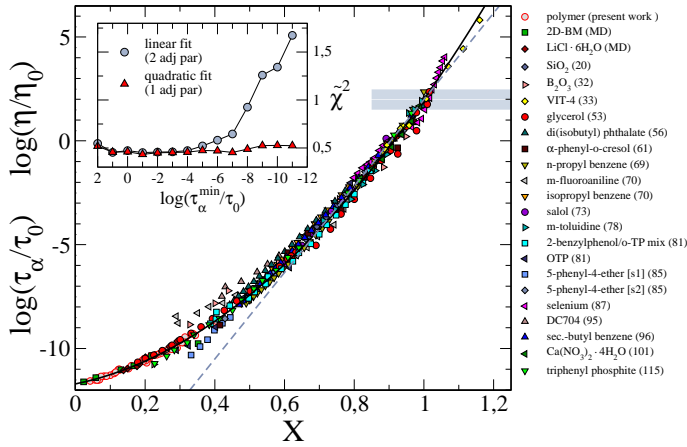


FIG. 3: (Color online) Scaling of the structural relaxation time and viscosity in terms of the reduced variable $X = G_r T_g / (G_r T)$. The continuous line is the quadratic form Eq.6. The dashed straight line is the linear form Eq.1 having replaced G_∞ with G_r . The numbers in parentheses denote the fragility of the systems (data sources in SM [20]). Data are considered only if the corresponding elastic moduli are measured at (angular) frequency $\omega > \max \{0.1/\tau_\alpha, 2\pi \cdot 1 \text{ MHz}\}$. Inset: χ^2 of the best-fit of the experimental data with both the quadratic form Eq.6 (allowing only the vertical shift of the experimental data [20]) and the modified Eq.1 (two adjustable parameters: the slope and the vertical shift). The fit spans the variable range from $\log \tau_\alpha^{\min}/\tau_0$ up $\log \tau_\alpha^{\max}/\tau_0 = 6$.

Fig.3 shows the comparison of Eq.6 with several systems spanning a wide range of fragilities and elastic moduli measured at sufficiently high frequencies to allow comparison with τ_α or η over wider ranges (elastic response is observed if $\omega\tau_\alpha \gg 1$). The experimental data are vertically shifted to adjust the conversion factor between MD and real units and ensure best-fit with Eq.6. No other adjustment is done. Data sources and related shifts are listed in SM [20]. Fig.3 shows that the modified Eq.1 with G_∞ being replaced by G_r results in a poorer fit in spite of the additional adjustable parameter (the slope). To get further insight, we calculated the chi-square of the two fits over the variable range from $\log \tau_\alpha^{\min}/\tau_0$ up $\log \tau_\alpha^{\max}/\tau_0 = 6$ (Fig.3 inset). It is seen that the two fits are equivalent in the range $-4 \leq \log \tau_\alpha \leq 6$ but Eq.6 performs much better in the range $-12 \leq \log \tau_\alpha \leq -4$. This is expected in that our analysis accounts for the competing effects of elastic trapping and anelastic escape, a feature which is missing in standard elastic models [7, 8].

In conclusion, we showed that plasticity cannot be neglected even on picosecond time scales where elastic effects seem to dominate the intermittent dynamics. The emerging quasi-elastic picture reveals the universal correlations between the residual elasticity left by intra-cage relaxation and the long-time relaxation due to cage breaking in a range of about eighteen decades in relaxation times, as well as clear connection to the underlying PEL.

S.Capaccioli and A. Ottochian are warmly thanked for sev-

eral discussions. Computational resources by "Laboratorio per il Calcolo Scientifico" (Physics Department, University of Pisa) are acknowledged.

* Electronic address: dino.leporini@df.unipi.it

- [1] C. A. Angell, K. L. Ngai, G. B. McKenna, P. McMillan, and S.W.Martin, J. Appl. Phys. **88**, 3113 (2000).
- [2] J.-P. Hansen and I. McDonald, *Theory of Simple Liquids*, 3rd Ed. (Academic Press, 2006).
- [3] E. R. Weeks and D. A. Weitz, Phys. Rev. Lett. **89**, 095704 (2002).
- [4] G. A. Appignanesi, J. A. Rodriguez Fris, R. A. Montani, and W. Kob, Phys. Rev. Lett. **96**, 057801 (2006).
- [5] C. De Michele and D. Leporini, Phys. Rev. E **63**, 036701 (2001).
- [6] A. V. Tobolsky, R. E. Powell, and H. Eyring, in *Frontiers in Chemistry*, edited by R. E. Burk and O. Grummit (Interscience, 1943), vol. 1, pp. 125–190.
- [7] J. C. Dyre, Rev. Mod. Phys. **78**, 953 (2006).
- [8] S. Nemilov, J. Non-Cryst. Sol. **352**, 2715 (2006).
- [9] B. Zhang, H. Y. Bai, R. J. Wang, Y. Wu, and W. H. Wang, Phys. Rev. B **76**, 012201 (2007); J. Mattsson, *et al.*, Nature (London) **462**, 83 (2009); D. H. Torchinsky, *et al.*, J. Chem. Phys. **130**, 064502 (2009); V. A. Khonik, *et al.*, Phys. Rev. B **79**, 132204 (2009); B. Xu and G. B. McKenna, J. Chem. Phys. **134**, 124902 (2011); M. L. Lind, G. Duan, and W. L. Johnson, Phys. Rev. Lett. **97**, 015501 (2006); M. D. Demetriou, *et al.*, Phys. Rev. Lett. **97**, 065502 (2006); S. V. Khonik, A. V. Granato, D. M. Joncich, A. Pompe, and V. A. Khonik, Phys. Rev. Lett. **100**, 065501 (2008); Y. P. Mitrofanov, *et al.*, J. Appl. Phys. **109**, 073518 (2011).
- [10] M. C. Ribeiro, J. Non-Cryst. Solids **355**, 1659 (2009).
- [11] J. Yang and K. S. Schweizer, J. Chem. Phys. **134**, 204909 (2011).
- [12] U. Buchenau, J. Chem. Phys. **131**, 074501 (2009).
- [13] A. Widmer-Cooper, *et al.*, Nature Physics **4**, 711 (2008); D. Ashton and J. Garrahan, Eur. Phys. J. E **30**, 303 (2009).
- [14] L. Larini, A. Ottochian, C. De Michele, and D. Leporini, Nature Physics **4**, 42 (2008); A. Ottochian, C. De Michele, and D. Leporini, J. Chem. Phys. **131**, 224517 (2009).
- [15] D. C. Wallace, *Thermodynamics of Crystals* (Wiley, New York, 1972).
- [16] K. Yoshimoto, T. S. Jain, K. Van Workum, P. F. Nealey, and J. J. de Pablo, Phys. Rev. Lett. **93**, 175501 (2004); C. E. Maloney and A. Lemaitre, Phys. Rev. E **74**, 016118 (2006); M. Tsamados, A. Tanguy, C. Goldenberg, and J.-L. Barrat, Phys. Rev. E **80**, 026112 (2009).
- [17] A. J. C. Ladd, *et al.*, J. Stat. Phys. **48**, 1147 (1987).
- [18] R. A. LaViolette and F. H. Stillinger, J. Chem. Phys. **83**, 4079 (1985).
- [19] J. H. van Zanten and K. P. Rufener, Phys. Rev. E **62**, 5389 (2000).
- [20] See Supplemental Material at [URL] for details about the model and the studied states, and the sources of the experimental data.
- [21] R. Zwanzig and R. Mountain, J. Chem. Phys. **43**, 4464 (1965).
- [22] K. L. Ngai, Phil. Mag. **84**, 1341 (2004).
- [23] A. S. Clarke and H. Jonsson, Phys. Rev. E **47**, 3975 (1993).
- [24] R. W. Hall and P. G. Wolynes, J. Chem. Phys. **86**, 2943 (1987).
- [25] $\langle u^2 \rangle^{-1}$ is proportional to the free-energy barrier for relaxation [11, 24]. Then, the elastic term and $\langle u_\infty^2 \rangle$ of Eq.2 are connected to the relevant energy and entropy costs, respectively.

- [26] F. W. Starr, S. Sastry, J. F. Douglas, and S. C. Glotzer, Phys. Rev. Lett. **89**, 125501 (2002).